Component Dynamics of a Miscible Polymer Blend: Polyisoprene and Polyvinylethylene

S. Adams and D. B. Adolf*

Department of Physics and Astronomy, University of Leeds, Leeds LS2 9JT, U.K.

Received October 29, 1998; Revised Manuscript Received February 24, 1999

ABSTRACT: Fluorescence anisotropy decay measurements were performed to determine the temperature and composition dependence of the local dynamics of each component of a miscible blend of high molecular weight polyisoprene (PI) and polyvinylethylene (PVE). The local dynamics of each component over the entire composition range from PI:PVE 0:100−100:0 was examined over the temperature range 20−100 °C. Optical measurements of the local dynamics of a probe chain in a matrix which is ∼100% the second polymer species are reported for the first time. Two blending rules for the temperature and composition dependence of the component dynamics are proposed, and their suitability to describe the observed local component dynamics is assessed. Different blending rules were found to be appropriate for the different blend components. A comparison to the work of Gisser and Ediger, describing solvent modification in polymer solutions, is also performed. The relative time scale of the motions of the two polymers in the blend is found to be linked to the rate at which the incorporation of a polymer additive influences the dynamics of the host polymer.

Introduction

The investigation of the component dynamics of polymer blends has received much attention in recent years. A wide variety of useful polymer properties can be obtained by blending two or more polymers. Understanding how the addition of one polymer, with known physical properties, to a second affects the overall properties of the resultant blend has been the driving force for much of this work.

The rheology of polymer blends is often complex, and time−temperature superposition has been shown to fail in many cases.[1−3] Several studies have shown that the rheological complexity may arise from the individual blend components possessing different temperature dependencies within the same blend matrix.[4,5] Although components can apparently maintain their distinct motional characteristics, they are sensitive to their environment, and blending has been shown to alter the dynamic time scale of both components within the blend.[4−7]

The effect of blending on the individual component dynamics has also been examined using the coupling scheme by Ngai.[8] Gisser and Ediger [9] have discussed the modification of solvent dynamics by a polymer solute within the bounds of the coupling scheme. They concluded that the extent to which the addition of the solute modifies the solvent dynamics is linked to the separation in time scales of the neat solvent motions and the solute motions at infinite dilution. Ngai and Rizos[10] have proposed an extension of this method to polymer blends in which the major blend component is considered to act as the solvent and the minor component as the solute.

In this study, fluorescence anisotropy decay measurements are made to examine the local segmental dynamics of both components of a polyisoprene (PI) polyvinylethylene (PVE) blend. Most high molecular weight polymers do not form miscible blends. Those that do are not usually stable over the entire composition and temperature range and two phase systems are often observed. High molecular weight blends of PVE with vinyl content >63% and PI are known to be miscible over the entire composition range and over all experimentally accessible temperatures.[11] The miscibility of this system is thought to be almost entirely entropically driven with $\Delta H \approx 0$.[12,13] The value of ΔH has actually been shown to be slightly negative but with a very small magnitude of the order 10^{-3}.[14] PI:PVE is therefore seen as a model system. Examining local dynamics in dilute solution has allowed access to the intrachain processes in the absence of interchain interactions. Concentrated solutions and measurements of local dynamics in bulk homopolymers have given information on the interchain processes. Using an athermal system such as this allows the most direct comparison between blended and unblended bulk dynamics without the complication of any effects due to specific interactions.

The key feature of the current optical technique is its sensitivity. The probe molecule need only be present to less than 0.5 wt %. The high sensitivity has enabled measurements of the dynamics of each component throughout the entire composition range. Measurements of the local dynamics of one species present in a matrix that is ∼100% the second polymer species are reported for the first time.

Method

Materials and Sample Preparation. Polyisoprene (PI) and polyvinylethylene (PVE, also known as 1,2-polybutadiene) blended samples were prepared by solvent casting. A typical sample contains approximately 400 mg of unlabeled polymer (PI and/or PVE) and <2 mg of one of the anthracene labeled probe species. The monodisperse unlabeled polymers were synthesized by Polymer Labs, and details of their microstructures and molecular weights are given in Table 1.

The probe molecules used in this study contained one anthracene chromophore covalently bonded in the middle of the chain; see the insets of Figure 1a,b and Table 1. Anthracene center labeled polyisoprene (PI*), synthesized at Durham University (Prof. R. Richards, Ms. A. Keeny, and Mr.

* To whom correspondence should be addressed. Tel 0113 2333812; Fax 0113 2333846.

10.1021/ma9816923 CCC: $18.00
Published on Web 04/15/1999

Table 1. Physical Characteristics of the Polymers Used in This Study

polymer	$M_w \times 10^{-3}$	polydispersity	microstructure		
			% cis-1,4	% trans-1,4	% vinyl-1,2
polyisoprene (PI)	89.9	1.02	91	9	0
polyvinylethylene (PVE)	129	1.03			86
anthracene labeled polyisoprene (PI*)	107	1.20	71	23	6
anthracene labeled polyvinylethylene (PVE*)	67.1	1.19			86

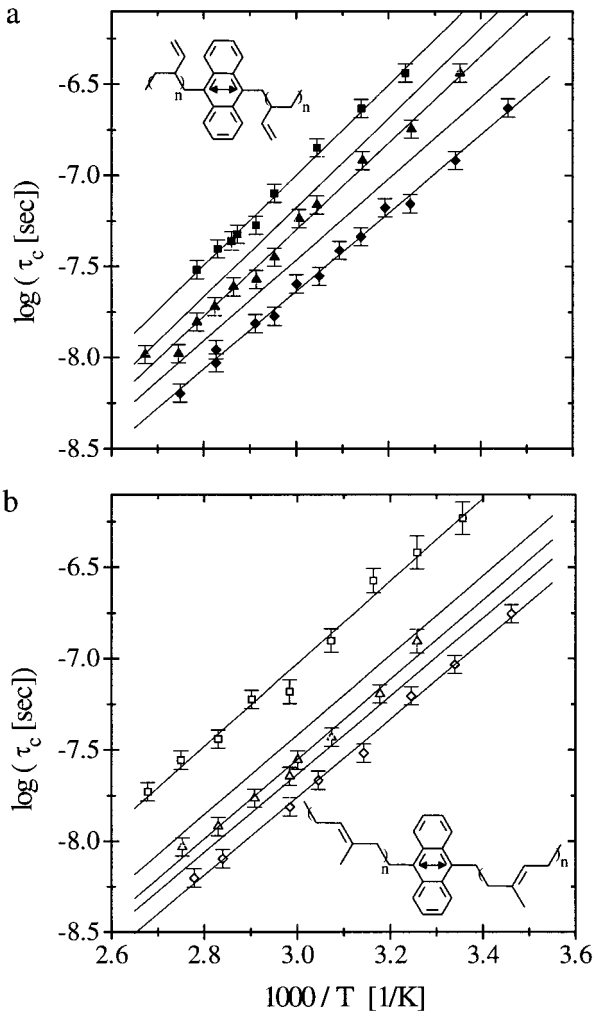

Figure 1. Correlation times for the component local dynamics of anthracene labeled polyvinylethylene, solid symbols (a), and polyisoprene, open symbols (b). The blend matrices are identified as PI:PVE: 0:100 (■), 50:50 (▲), and 100:0 (◆). The data for the 25:75 and 75:25 samples have been omitted for clarity, and only the line of the best fit is shown. The experimental scatter in the data points for these samples is similar to the scatter of the samples shown. The slope of each line of best fit for each blend is related to the experimental activation energy. The insets show the structure of the labeled polymer used in each case. The $S_0 \rightarrow S_1$ electronic transition dipole moments are indicated by the doubled-headed arrows.

T. Keef), and anthracene center labeled polyvinylethylene (PVE*), from Polymer Labs, were used to monitor the dynamics of the PI and PVE components, respectively. The $S_0 \rightarrow S_1$ electronic transition dipole moment, the doubled-headed arrow of the insets of Figure 1, of the anthracene chromophore is orientated along the chain backbone; hence, any movement of the dipole reflects movement of the polymer backbone.

Solutions of all four polymers were made up in toluene (Aldrich, >99.5% purity) and then mixed in the appropriate proportions. The solutions were subject to several freeze−pump−thaw cycles to replace molecular oxygen with molecular nitrogen and allowed to stand under nitrogen to become fully homogenized. The solutions were then removed to a nitrogen atmosphere and drop cast onto $^1/_2$ in. optical flats. Repeated applications were made to build up a sample 1−2 mm in thickness. Once all the visible solvent had evaporated into the nitrogen atmosphere, the last traces of toluene were removed by leaving the sample under vacuum for ∼7 weeks.

Solutions were mixed so as to generate blended samples in the range PI:PVE 0:100−100:0, each containing <0.5 wt % of either PI* or PVE*. The weight fraction of labeled polymer introduced was based on the concentration required to give an OD of <0.1 in a 3 mm path length of a dilute solution. The nomenclature used throughout this paper refers to blends as a weight ratio of PI to PVE. The component dynamics being monitored, that is the species for which a small proportion of the whole consists of the labeled polymer, is denoted by an asterisk. For example, a blend containing 25% PI and 75% PVE of which <0.5% is the labeled PVE* is denoted 25:75*. The errors in the compositions quoted are ≤2%.

A series of experiments were conducted to ensure that all the solvent was removed from the samples during the period under vacuum. A 100*:0 sample was prepared. The segmental dynamics of this sample were measured after different periods under vacuum. The correlation times for the dynamics were found to be constant to within experimental error after 5 weeks under vacuum. After this time, the sample was assumed to be free of solvent. The final correlation times for this sample was found to agree with the work of Hyde et al., where the dynamics were found to follow the temperature dependence of the macroscopic steady shear viscosity of a PI sample of similar microstructure and molecular weight.[15] All data reported in this paper were collected from samples that had been held under vacuum for a minimum period of 7 weeks.

Experimental Technique. Fluorescence anisotropy decay (FAD) data were collected using the method of time-correlated single photon counting (TCSPC). The experimental technique and method of data acquisition have been described in detail elsewhere,[16] and only a brief description is given here. The experimental apparatus has been described elsewhere.[17]

A short (∼5 ps) linearly polarized pulse of laser light at 406 nm was used to photoselect an anisotropic distribution of anthracene chromophores. These chromophores emit light that is polarized along the $S_0 \rightarrow S_1$ electronic transition dipole moment. Hence, the emission from the samples was initially partially polarized. Molecular motions of the polymer backbone randomize the orientations of the excited-state chromophores and depolarize the emission. The reorientation of the transition dipoles is observed by monitoring the components of the fluorescence decay polarized parallel, $I_{||}$, and perpendicular, $I_{\perp}$, to the excitation radiation. Fluorescence was collected at 414 nm.

The time-dependent anisotropy, $r(t)$, is constructed from the measured decays as

$$r(t) = \frac{I_{||}(t) - I_{\perp}(t)}{I_{||}(t) + 2I_{\perp}(t)} \tag{1}$$

This describes the time dependence of the reorientation of the excited-state chromophores and is directly related to a second-order orientation autocorrelation function, $CF(t)$,

$$r(t) = r_0 CF(t) \tag{2}$$

which describes the average reorientation of the transition dipole between the times of excitation and emission through

$$CF(t) = \langle P_2(\cos\theta(t))\rangle \quad (3)$$

P_2 is the second Legendre polynomial, and $\theta(t)$ is the angle through which a transition dipole moment has rotated in a time t since the excitation pulse. The angular brackets indicate an ensemble average over all the excited-state transition dipole moments. Thus, the observation of $I_{\parallel}(t)$ and $I_{\perp}(t)$ allows the direct calculation of the orientation autocorrelation function without the assumption of any motional model.

Data Analysis. The distortions introduced into the data by the finite duration of the laser pulse and the response of the detection equipment were deconvolved from the data during analysis by an iterative reconvolution process. The anisotropy decays were fitted to either one or both of two functions, the generalized diffusion and loss (GDL) model[18] (eq 4), as has been adopted in previous studies of bulk dynamics,[15,19,20] or an empirical biexponential (BE) function (eq 5).

$$r(t) = r_0 \exp(-t/\tau_1)\exp(-t/\tau_2)[I_0(t/\tau_1) + I_1(t/\tau_1)] \quad (4)$$

$$r(t) = A\exp(-t/\tau_3) + B\exp(-t/\tau_4) \quad (5)$$

The quantities τ_1, τ_2, τ_3, τ_4, r_0, A, and B (where $A + B = r_0$) are fitting parameters, and I_0 and I_1 are the zeroth- and first-order modified Bessel functions, respectively. The parameters τ_1 and τ_2 are related to the correlated and uncorrelated motions described by Helfand.[21] No physical significance is placed on the parameters τ_3 and τ_4. In the current work only the overall time scale of the motions is of interest. Equation 6 defines a model-independent parameter, the correlation time of the decay, which can be obtained from both expressions. Equation 6a gives the result of applying the integral of eq 6 to the GDL model, and eq 6b gives the correlation time of the BE expression.

$$\tau_c = \int_0^\infty CF(t)\,dt = (1/r_0)\int_0^\infty r(t)\,dt \quad (6)$$

$$\tau_c = \{2/\tau_1\tau_2 + 1/\tau_2^2\}^{-1/2} \times [(1/\tau_1)\{1/\tau_1 + 1/\tau_2 + (2/\tau_1\tau_2 + 1/\tau_2^2)^{1/2}\}^{-1} + 1] \quad (6a)$$

$$\tau_c = (A\tau_3 + B\tau_4)/(A + B) \quad (6b)$$

At high temperatures, the dynamics are fast and the correlation times, τ_c, calculated from both the GDL and BE models are in agreement. At lower temperatures, the correlation times become longer, and only a limited fraction of the anisotropy decay can be seen in the experimental time window. In this regime, the BE expression fails to capture the true shape of the decay, reducing to what is effectively a single-exponential fit with $\tau_3 \approx \tau_4$. The correlation time is consequently underestimated by the BE expression for the slower dynamics. Correlation times in excess of ~60 ns cannot be reliably obtained from this fitting method. The GDL expression can be used out to these longer correlation times by constraining the ratio of the fit parameters τ_2/τ_1, and so constraining the shape of the decay, to be equal to that found from the higher temperature measurements, 5 ± 2. Previous studies examining the bulk dynamics of a variety of polymers have also found that τ_2/τ_1 shows no systematic variation with temperature and can be constrained to the average value found from fits at higher temperatures.[15,20,21] The method of constrained fitting was not appropriate for the simple BE function as it was not possible to predict the low-temperature ratio of τ_4/τ_3 from the temperature dependence observed at higher temperatures. The correlation times reported here were calculated from either the BE or GDL expressions as appropriate.

The quality of the fits is assessed in terms of the r_0 value and the reduced chi squared value, χ^2_R. The average r_0 of the current work was 0.30 ± 0.04 over all temperatures and compositions, in good agreement with previous studies of anthracene labeled polymers.[17,22,23] Typical χ^2_R values were in the range 1.0−1.3. Measurements were made on different days and/or samples, and data were found to be reproducible to within 10−15%.

Table 2. Glass Transition Temperatures, WLF Coefficients, and Apparent Arrhenius Activation Energies for Each Blend Studied[a]

blend	T_g [K]	C_1^g [b]	C_2^g [b] [K]	E_a [kJ mol^{-1}]
Labeled PVE Dynamics				
0:100*	255 (6)	11.4	56	47.5 ± 1.4
25:75*	242 (23)	11.8	55	47.0 ± 1.7
50:50*	225 (19)	11.8	55	45.5 ± 1.4
75:25*	215 (6)	11.8	55	42.6 ± 1.0
100:0*	210 (5)	11.8	52.9	41.1 ± 0.9
Labeled PI Dynamics				
0*:100	255 (5)	11.4	56	43.4 ± 1.8
25*:75	238 (21)	11.8	55	41.8 ± 0.8
50*:50	224 (18)	11.8	55	41.8 ± 2.2
75*:25	217 (6)	11.8	55	41.0 ± 1.9
100*:0	209 (4)	11.8	52.9	40.9 ± 1.0

[a] The number in parentheses after the glass transition temperature indicates the breadth of the transition. [b] Values taken from ref 5.

Results

The measured correlation times for the local dynamics of PVE* and PI* in the different blend matrices are shown in Arrhenius format in parts a and b of Figure 1, respectively. The observed correlation times cover approximately 2 decades in time. As expected, the slowest dynamics for each component occur in an all PVE matrix, the higher T_g component, and the fastest in an all PI matrix, the lower T_g component. The activation energy for local dynamics of each component within each blend is calculated from the slope of each line of best fit in Figure 1. The values are given in Table 2. There is a general trend toward an increase in activation energy with increasing PVE content of the blend. It can also be seen from Table 2 that the activation energies for the PVE* dynamics are generally higher than those for the PI* dynamics in the same host matrix. This difference is most apparent in blends with high PVE content.

Isothermal plots, at 90, 60, and 30 °C, of log correlation time as a function of blend composition are shown in Figure 2. Here, the correlation times at constant temperature, obtained from the straight line fits of Figure 1, are plotted against blend composition. It can be seen that, in all cases, the correlation time for the PVE component, τ_{pve}, is greater than that of the PI component, τ_{pi}. The difference between τ_{pve} and τ_{pi} is exaggerated in the blended samples in the middle of the composition range. In the extreme cases, the 0:100 and 100:0 matrices, the component dynamics are much less widely separated, especially in the all PVE matrix, where both PI* and PVE* demonstrate very similar motional time scales. For the PVE component, a smooth progression to higher correlation times with increasing PVE content is observed. For PI*, there is an abrupt increase in correlation time between the 25*:75 and the 0*:100 systems. This abrupt increase is also evident in Figure 1b.

Discussion

Temperature Dependence. The temperature dependence of the data was examined in terms of the WLF equation[24]

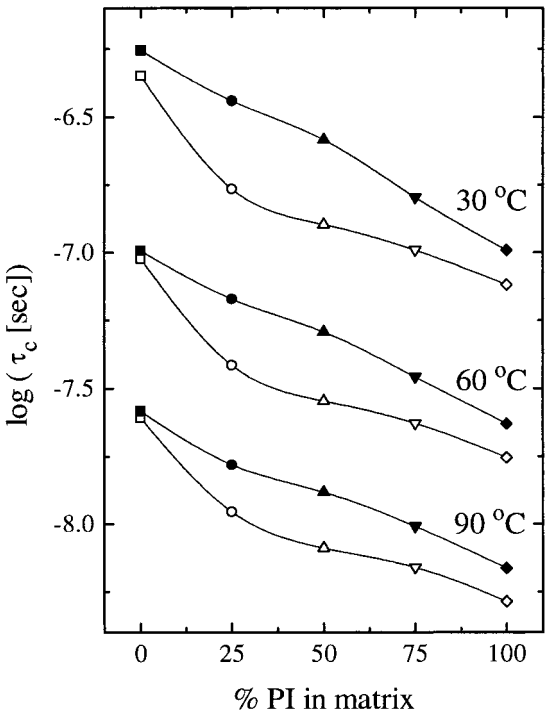

Figure 2. Isothermal plots showing the composition dependence of the local component dynamics. The blend matrices are identified as PI:PVE: 0:100 (■), 25:75 (●), 50:50 (▲), 75:25 (▼), and 100:0 (◆) with solid symbols representing PVE dynamics and open symbols PI dynamics.

$$\log(\tau_c) = \log(\tau_g) - \frac{C_1^g(T - T_g)}{C_2^g + (T - T_g)} \tag{7}$$

where τ_g is the correlation time of the dynamic at the glass transition temperature, T_g, and C_1^g and C_2^g are polymer-dependent constants. For PI and PVE, C_1^g and C_2^g are similar, and values for the blended samples do not alter much from the pure component values.[5] The values of C_1^g and C_2^g used were taken from ref 5 and are given in Table 2. Once fluorescence data had been collected, the glass transition temperature of each blend was measured on a Perkin-Elmer DSC7 at a heating rate of 10 °C min^{-1}. The measured T_g values are also given in Table 2. The slight difference in the measured T_g for samples of the same blend ratio arises due to a ±2% uncertainty in the blend composition and from uncertainties due to the breadth of the transitions indicated by the number in brackets of Table 2. Figure 3 shows the data plotted against the relative temperature $1/(T - T_g)$.[25] The solid lines in the plots indicate WLF fits to the PVE component dynamics and the dotted lines to the PI component dynamics. The only free parameter in the fitting procedure was $\log(\tau_g)$, amounting to only a vertical shift. The shape of the curve as dictated by the temperature dependence is fixed by the choice of C_1^g, C_2^g, and T_g. Figure 3 shows reasonable agreement of the WLF equation and the data for the low PVE content blends using the macroscopic blend T_g in all cases. For these blends, however, the data were collected in the region $T \geq T_g + 80$. In this regime, there is very little curvature and the WLF equation approximates to a straight line, equivalent to an Arrhenius fit. Measurements closer to T_g were taken for blends with higher PVE content. Figure 3 clearly shows a failure of WLF behavior for these blends with large deviations from the predicted behavior. Previous studies predict WLF behavior in the blends is only obeyed when individual component T_g's are considered. The WLF fits obtained for the low PVE content blends all show good agreement using the macroscopic blend T_g. Further, no realistic component T_g values could be found which improved the agreement for the high PVE content blends.

The Arrhenius fits to the data adequately describe all the data over the given temperature range. These fits do show a composition-dependent temperature dependence through the different activation energies reported in Table 2. Further to this, the different components show a different temperature dependence within the same blend. These findings are consistent with those of previous studies,[4,5,7] although the absolute form of the temperature dependence is not WLF in this temperature regime.

Composition Dependence. The influence a polymer additive has on the dynamics of the host polymer is not well understood. Many empirical blending rules exist to describe the macroscopic properties of blend samples.[4,26] An analogy is drawn from rules proposed for systems in which there are two, widely separated dynamic time scales, such as concentration and density fluctuations of blends of polymers with a high T_g contrast.[27] Equations 8 and 9 are proposed in this study as microscopic analogues to these rules.

$$\tau_1(T) = \phi_1\tau_{1,1}(T) + \phi_2\tau_{1,2}(T) \tag{8}$$

$$\frac{1}{\tau_1(T)} = \frac{\phi_1}{\tau_{1,1}(T)} + \frac{\phi_2}{\tau_{1,2}(T)} \tag{9}$$

where τ_1 refers to the correlation time of component 1 in a given blend. $\tau_{1,1}$ refers to a correlation time characteristic of a labeled 1-molecule in a matrix of all unlabeled 1-molecules. $\tau_{1,2}$ refers to a correlation time characteristic of a labeled 1-molecule in a matrix that is 100% unlabeled 2-molecules. ϕ_i refers to the weight fraction of species i. Using the weight fraction, as opposed to the number fraction of carbon atoms, gives ≤1% difference in the actual value of ϕ_i, which is well within the experimental uncertainty. The series combination, eq 8, is most heavily influenced by the dynamics of the slower component in the blend, whereas the parallel combination is more heavily influenced by the faster of the two components. Each of these rules will now be considered in turn.

Series. Equation 8 is compared to the data using no free parameters. $\tau_{1,1}$ is expressed in Arrhenius format, $\tau_{1,1} = A\exp(E_a/RT)$, where A and E_a for $\tau_{pi,pi}$ are obtained from fits to 100*:0 data. A and E_a for $\tau_{pve,pve}$ are obtained from fits to 0:100* data. $\tau_{1,2}$ is similarly expressed in an Arrhenius form, $\tau_{1,2} = A'\exp(E_a'/RT)$, with A' and E_a' taken from fits to the data for a labeled 1-molecule, in a matrix that was 100% species 2. Hence, $\tau_{pi,pve}$ is taken from fits to 0*:100 and $\tau_{pve,pi}$ from fits to 100:0*. It is apparent from this definition of $\tau_{1,2}$ that $\tau_{pi,pve}$ is not necessarily equal to $\tau_{pve,pi}$.

The temperature dependencies of the measured blend dynamics of PVE, τ_{pve}, and PI, τ_{pi}, are compared to the predictions of eq 8, using the $\tau_{1,1}$ and $\tau_{1,2}$ values described above, in Figure 4, a and b, respectively. The symbols of this figure represent the measured data points and the solid lines the predictions of eq 8.

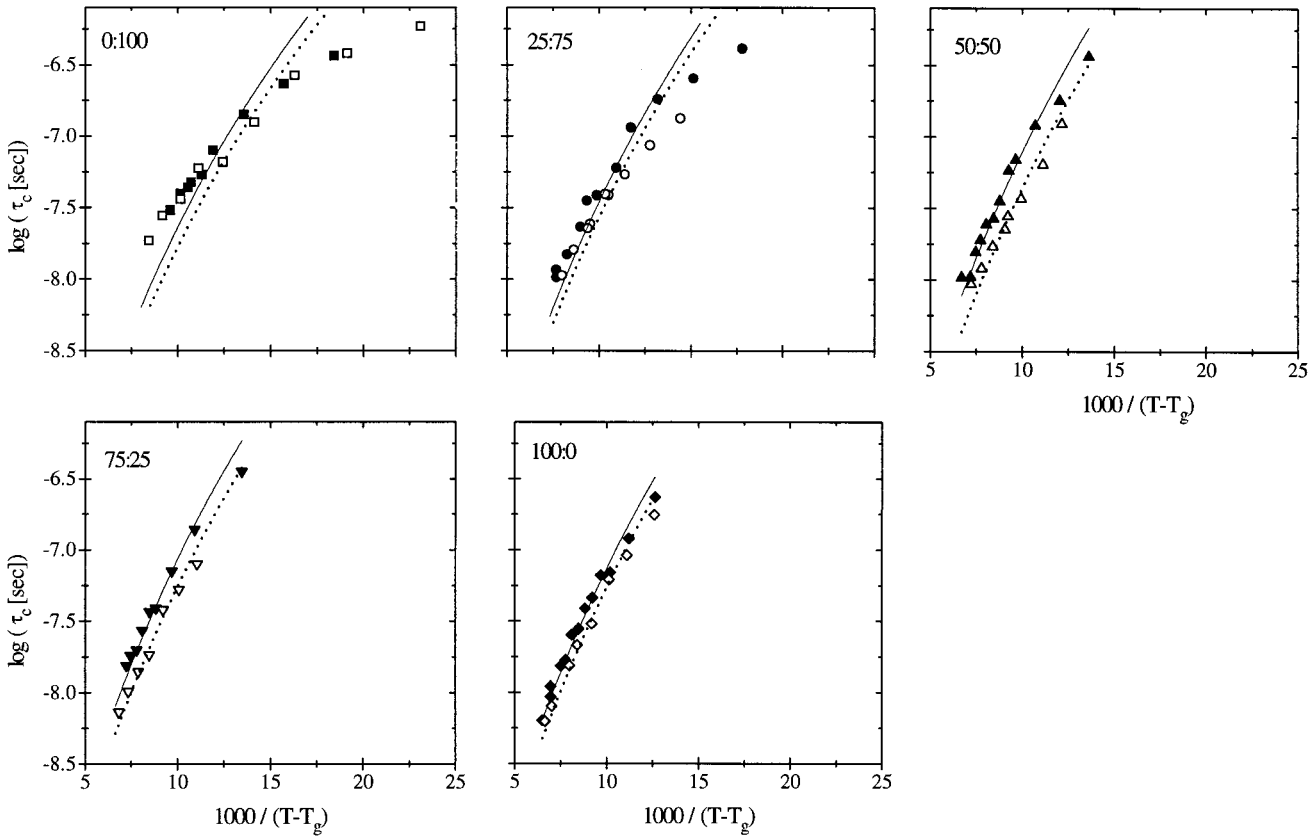

Figure 3. WLF fits to the data. The macroscopic blend T_g was used with the WLF coefficients given in Table 2. The blend matrix is given as a ratio PI:PVE in the top left of each plot. The symbols are the same as those for Figure 2. The solid lines represent fits to the PVE component data and the dotted lines fits to the PI component.

It can be seen from Figure 4a that this simple additive approach captures the behavior of the local blend dynamics of the PVE component well. Figure 4b demonstrates that this approach fails for the blended dynamics of the PI component. The solid line lies above the open symbols for each of the blended samples, showing that the observed blended PI dynamics are significantly faster than is predicted by this simple approach.

For the case of the PI local component dynamics, a second attempt is made to find an expression similar to eq 8 which can describe the behavior observed in Figure 4b. Since the dynamics predicted by eq 8 in the form described above are much slower than the measured dynamics, the dominant slow term of the expression is examined. The Arrhenius format of $\tau_{pi,pve}$ is held constant, but the parameters A' and E'_a are treated as fitting parameters and allowed to vary for each blend composition. Fits were performed to the data from 25*:75, 50*:50, and 75*:25 samples. The values of A' and E'_a obtained for all blend compositions were the same to within experimental uncertainty, falling in the range 11.7 ± 2.5 fs and 41.8 ± 0.2 kJ mol^{-1}, respectively. The average values for A' and E'_a obtained from these fits are used to generate a single expression for the temperature dependence of $\tau_{pi,pve}$ independent of blend composition, $\tau_{pi,pve}$(blend). This $\tau_{pi,pve}$(blend), rather than the directly measured $\tau_{pi,pve}$, is used in conjunction with the $\tau_{pi,pi}$ used previously to generate the dotted lines of Figure 4b. The effect of using this average value rather than rather than the measured value of $\tau_{pi,pve}$ is clearly seen when the solid and dotted lines of the 0*:100 panel of Figure 4b are compared. $\tau_{pi,pve}$(blend) predicts much faster dynamics than are actually observed for labeled PI in bulk PVE. It can be seen from the agreement between the open symbols and the dotted lines of Figure 4b that this single expression for $\tau_{pi,pve}$(blend) is sufficient to describe the behavior of the PI component in each of the blends studied. That a single expression for $\tau_{pi,pve}$(blend) can be used to capture the behavior of the PI component in all the blends studied is perhaps surprising in light of the sensitivity of eq 8 to changes in A' and in particular E'_a. The difference in the E'_a values used to generate the solid and dotted lines of Figure 4b is only 4% but leads to a large difference in the values of τ_{pi} generated.

In all the blended systems studied over the temperature range of the current experiments, the blend dynamics can be predicted using eq 8 and two correlation times $\tau_{1,1}$ and $\tau_{1,2}$. The $\tau_{1,1}$ correlation time is derived from the dynamics of the bulk homopolymer. For the PVE component local dynamics, the second correlation time, $\tau_{1,2}$, is derived from the motions of the PVE probe in a matrix of bulk PI. For the PI component local dynamics, the $\tau_{1,2}$ term is not taken from PI* in bulk PVE but can deduced from any one of the blended samples. This picture is consistent with the observation that the PVE component dynamics are slower than the PI component dynamics, and hence the PVE component senses only a time-averaged value for the PI relaxation, independent of whether the PVE dynamics are monitored in a blended sample or a matrix of all PI. This is not true for the faster PI component where, for the range of blend compositions studied, the value of $\tau_{1,2}$ is found to depend on whether the probe is present in a blended sample (independent of blend composition) or a matrix of all PVE.

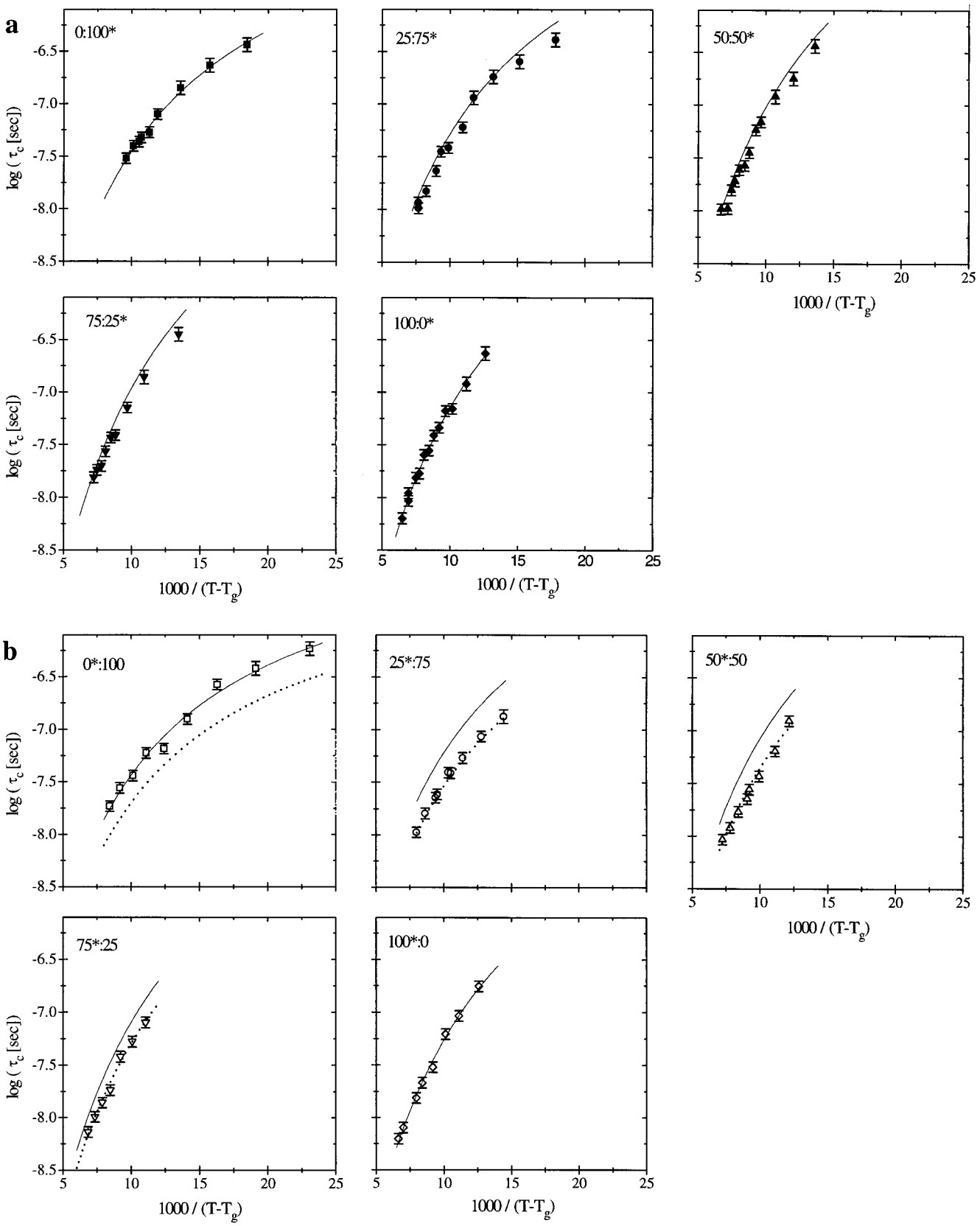

Figure 4. Comparison of the measured correlation times, the symbols, to the predictions of eq 8, $\tau_1 = \phi_1\tau_{1,1} + \phi_2\tau_{1,2}$, the lines. The symbols are as for Figure 2, and the blend sample name is given in the top left corner of each plot. $\tau_{1,1}$ is taken from measurements of the labeled species in its own host matrix. The solid lines represent the function with $\tau_{1,2}$ taken from measurements of the labeled polymer in a host matrix that is ~100% the other polymer species. The dotted lines of (b) represent the function with $\tau_{1,2}$ taken as the average value for which the function captures the blend behavior of PI. This value of $\tau_{1,2}$ is the same for all three blend cases of (b).

Parallel. We now compared the predictions of eq 9 to the measured data using no free parameters. $\tau_{1,1}$ and $\tau_{1,2}$ are used in the unmodified form, taken from Arrhenius fits of the probe (1-molecule) dynamics in

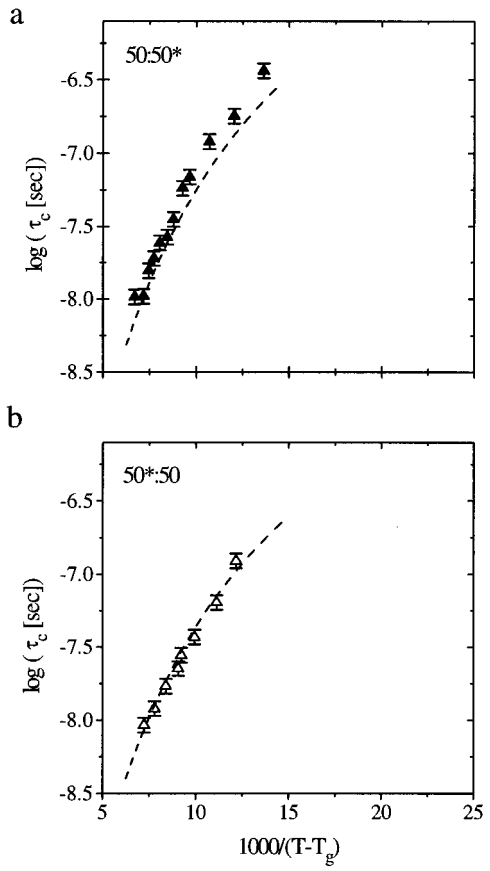

Figure 5. Comparison of the measured correlation times, the symbols, to the predictions of eq 9, $\tau_1^{-1} = \phi_1\tau_{1,1}^{-1} + \phi_2\tau_{1,2}^{-1}$, the dashed lines, for the 50:50 blend. The solid symbols represent PVE* dynamics and the open symbols PI* dynamics. $\tau_{1,1}$ is taken from measurements of the labeled species in it own host matrix, and $\tau_{1,2}$ is taken from measurements of the labeled species in a host matrix that is ~100% the other polymer species.

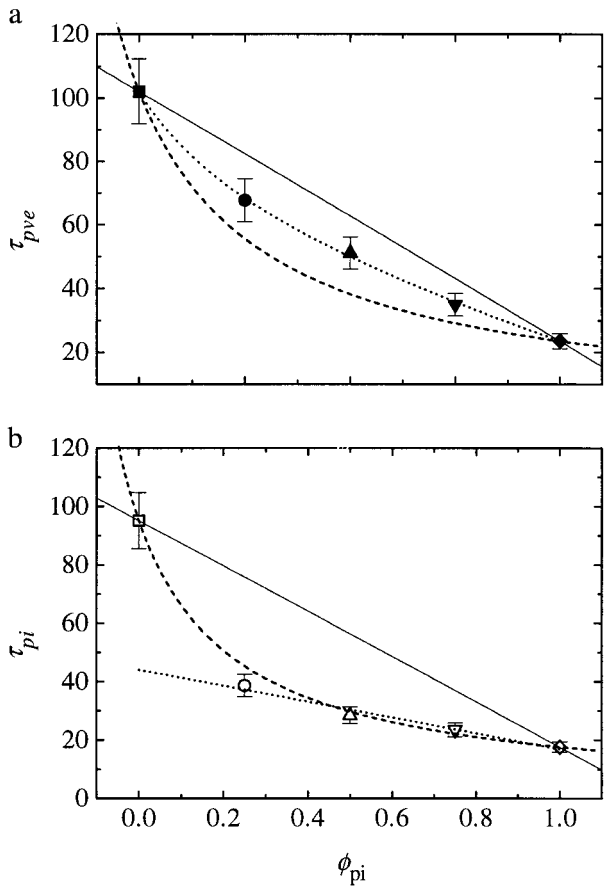

Figure 6. Comparison of the measured local component dynamics of PVE (solid symbols) and PI (open symbols) to the series (solid lines) and parallel (dashed lines) blend expressions. The dotted line of (a) is a linear combination of the series and parallel expressions. The dotted line of (b) is a linear fit through the data points for high PI content blends (≥25% PI).

each of the bulk homopolymer matrices (1- and 2-molecules, respectively). Examples of the comparison of the temperature dependencies of the measured dynamics of PVE, τ_{pve}, and PI, τ_{pi}, and the predictions of eq 9 are shown for the 50:50 blend in parts a and b of Figure 5, respectively. The symbols represent the measured data and the dashed lines the predictions of eq 9.

It can be seen from Figure 5b that the parallel approach captures the behavior of the PI component dynamics without the need for the modification of any of the parameters. The agreement for all the blend samples is very close using the measured quantities $\tau_{1,1}$ and $\tau_{1,2}$ and eq 9. Figure 5a also demonstrates reasonable agreement between the measured blend dynamics of PVE and the predictions of eq 9, although, in all cases, the prediction is systematically slightly faster than the measured quantity.

The composition dependence of the both rules is compared to the measured data at a constant temperature of 60 °C in Figure 6. Again, the symbols represent the measured data and the solid lines represent the series combination, eq 8, while the dashed lines represent the parallel expression, eq 9.

Figure 6b shows good agreement between the observed PI component dynamics and the parallel expression, the dashed line, using only the measured values of $\tau_{pi,pi}$ and $\tau_{pi,pve}$ with no modification. The unmodified series expression, the solid lines, clearly fails in the PI case. The reason for the apparent agreement with the series expression when $\tau_{pi,pve}$(blend) is used becomes apparent when only the blended samples are examined. Due to the approximate linearity of the curve over the range of blended samples investigated, an apparent linear fit can be made to the data by ignoring the point of PI* in bulk PVE, the dotted line of Figure 6b. The value of $\tau_{pi,pve}$ predicted from this straight line fit is in agreement with the value of $\tau_{pi,pve}$(blend) at this temperature obtained from the modified series analysis. The form of the parallel expression is also seen to predict the abrupt change observed between the PI* dynamics in the 25:75 blend and in bulk PVE (see Figure 1b). It would be interesting to investigate the component dynamics in blends covering the composition range from 25:75 to 0:100, to enable a more stringent comparison between measurements and the predictions of the parallel expression in the vicinity of the curved portion of the dashed line.

The dashed and solid lines of Figure 6a fall close to the measured data on either side, showing that either expression can be used to approximately predict the blend dynamics. The dotted line, which accurately captures the observed behavior, is a simple linear combination of the series and parallel expressions, eq 10.

$$\tau_{pve} = a\tau_{series} + b\tau_{parallel} \qquad (10)$$

Several plot similar to those of Figure 6 have been

constructed at various temperatures throughout the experimental temperature range. In all cases, the PI behavior was accurately captured by the parallel expression only. To accurately capture the PVE* dynamics, the use of eq 10 was required in all cases. For all the temperatures investigated, $a + b$ was found to be equal to 1 ± 0.02 where the value of a decreases, from 0.5 to 0.40, and hence b increases, from 0.5 to 0.60, with increasing temperature over the range 20−90 °C.

Comparison to Solvent Modification in Polymer Solutions. The effect on a solvent's dynamics of introducing a polymer additive to the solvent has been investigated by many authors.[8,9,28,29] The addition of a polymer can act to either slow down or speed up the solvent dynamics. The concentration dependence of solvent dynamic modification has been found experimentally to follow an approximate exponential form (eq 11).

$$\frac{\tau_{solv}(c_{poly},T)}{\tau_{solv}(c_{poly}=0,T)} \approx \exp(A_{poly}c_{poly}) \qquad (11)$$

τ_{solv} is the measured relaxation time of the solvent in solution with the concentration of dissolved polymer given by c_{poly}. The ratio of the correlation time for solvent dynamics in the solution to the correlation time in the neat solvent is a measure of the solvent modification. The parameter A_{poly} can be either positive or negative and describes the rate of solvent dynamic modification on addition of polymer. A_{poly} is independent of polymer concentration and carries all of the temperature dependence of the ratio.

The sign and magnitude of A_{poly} depend on the specific polymer−solvent system under investigation and on the temperature. Polystyrene (PS) in Aroclor, for example, has a small positive A_{ps} value, indicating that the solvent dynamics are slower in solution than in the neat solvent. 1,4-Polybutadiene (PB) in Aroclor, on the other hand, has a negative A_{pb} with a somewhat larger magnitude, indicating that the solvent dynamics are faster in solution than in neat solvent and that the rate at which the solvent dynamics speed up as PB is added is greater than the rate of slowing down due to the addition of PS.

Gisser and Ediger linked this solvent modification to the relative time scales of the polymer and solvent motion through eq 12.[9]

$$\frac{\partial}{\partial c_{poly}} \ln \frac{\tau_{solv}(c_{poly},T)}{\tau_{solv}(c_{poly}=0,T)} = A_{poly} = Q_{poly} \log \frac{\tau_{poly}(c_{poly} \to 0,T)}{\tau_{solv}(c_{poly}=0,T)} \qquad (12)$$

τ_{poly} is the measured relaxation time for the polymer dynamics. The ratio on the right compares the correlation time for the local polymer dynamics in dilute solution to those of the neat solvent. Q_{poly} is an adjustable constant of proportionality and contains information on the extent of coupling of the solvent dynamics to their solution environment.

Ngai and Rizos have proposed that the above description of polymer solutions can be adapted for use with polymer blends by treating the majority component as the solvent and the minority component as the solute.[10] Alegria and co-workers[30] have examined dielectric data from PI:PVE blends in this way. The current optical data is analyzed in terms of eqs 13a and 13b, analogous to the solution eqs 11 and 12.

$$\frac{\tau_1(c_2,T)}{\tau_1(c_2=0,T)} \approx \exp(A_2c_2) \qquad (13a)$$

$$\frac{\partial}{\partial c_2} \ln \frac{\tau_1(c_2,T)}{\tau_1(c_2=0,T)} = A_2 = Q_2 \log \frac{\tau_2(c_2 \to 0,T)}{\tau_1(c_2=0,T)} \qquad (13b)$$

In the case where PI is treated as the solvent, 1 = PI and 2 = PVE. In the case where PVE is viewed as the solvent, 1 = PVE and 2 = PI. In the previous analysis of the dielectric data, Q_{pi} and Q_{pve} could not be compared directly to the solution case, Q_{poly} since no blend measurements were available that were directly analogous to the dilute solution case, where $c_2 \to 0$. Here, a critical analysis is performed on the magnitude of Q_2 as a function of the composition of the blend selected to determine the numerator of the ratio $\tau_2(c_2 \to 0,T)/\tau_1(c_2 = 0,T)$.

Plots were constructed of $\ln[\tau_1(c_2,T)/\tau_1(c_2 = 0,T)]$ against c_2 at several temperatures in order to generate an A_2 value at each of these temperatures. According to eqs 13a and 13b, these plots should be straight lines through the origin with slopes given by A_2. When the subscript 1 refers to PI (1 = PI) and the subscript 2 to PVE (2 = PVE), A_{pve} is generated. When 1 = PVE and 2 = PI, A_{pi} is generated. The values of the correlation times, τ_1, used to construct the ratios were taken from the Arrhenius fits to the data. Ratios were created at various points throughout the entire experimental temperature range. These plots for the 1 = PVE case were approximately linear over all concentrations, c_{pi}, in the range 0−100%. The values for A_{pi} were thus taken as the slope of the best fit line through the origin. The corresponding plots used to generate A_{pve} (the case 1 = PI) were only approximately linear over a restricted concentration range, 0−75% PVE. PI dynamics in a matrix of 100% PVE deviate strongly from the straight line predicted by the lower PVE content samples. It is noted that Ngai and Rizos report values of A_2 which are concentration-dependent. These points indicate that the exponential form of the concentration dependence from the polymer solution experiments is not strictly observed for polymer blends. However, the composition at which the current data deviate from exponential behavior is above the concentration ranges used in the solution experiments, and the deviation may be due to the high concentrations. The values of A_{pve} reported were obtained from straight-line fits to only the linear portion of the curve. Values of A_{pi} and A_{pve} were obtained at several temperatures in the range 20−80 °C.

The values obtained for A_{pi} and A_{pve} are plotted as a function of temperature in Figure 7 as open (A_{pi}) and solid (A_{pve}) squares. The values reported by Ngai and Rizos are also shown as the open and solid triangles. Although the data were collected using different experimental techniques over different temperature ranges, excellent agreement is found between the two studies. The A_{pi} values of the current study (open squares) compare well with those obtained from the dielectric data (open triangles). Similarly, the solid symbols representing A_{pve} all appear to follow a single smooth curve.

Gisser and Ediger found that, for polymer solutions, the temperature dependence of A_{poly} followed the same form as that for the log of the ratio of the dilute solution

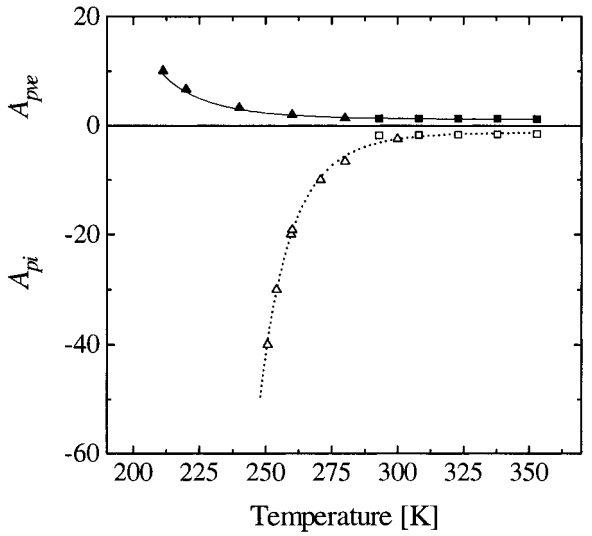

Figure 7. Plot showing the temperature dependence of A_{pi} and A_{pve} from $A_2 = \partial \ln[\tau_1(c_2,T)/\tau_1(c_2 = 0,T)]/\partial c_2$. Open symbols refer to A_{pi} and solid symbols to A_{pve}. The squares represent the current optical data and the triangles the dielectric data of ref 10. The lines are a guide to the eye.

Table 3. Q_2 Values Obtained from Plots of A_2 vs $\log[\tau_2(c_2,T)/\tau_1(c_2 = 0,T)]$ Using the $\tau_2(c_2)$ Values Indicated To Generate the Ratio $\tau_2(c_2,T)/\tau_1(c_2 = 0,T)$

Q_2 values calcd using	"solvent"	τ_2 ($c_2 \approx 0$)	τ_2 ($c_2 = 25\%$)	τ_2 ($c_2 = 50\%$)	τ_2 ($c_2 = 75\%$)
Q_{pi}	PVE	20 ± 5	3.9 ± 0.9	3.0 ± 0.6	2.5 ± 0.2
Q_{pve}	PI	10 ± 3	4.1 ± 0.8	2.6 ± 0.8	2.0 ± 0.6
Q_{pi}(Ngai)	PVE			1.6	
Q_{pve}(Ngai)	PI		1.3		
Q_{poly}	Aroclor[a,b]	≈4			
Q_{poly}	toluene[a,c]	<1.4			
Q_{poly}	THF[a,c]	≤0.5			

[a] Values taken from ref 9. [b] Based on data from polystyrene, polyisoprene, and polybutadiene solutions. [c] Based on data from polystyrene solutions.

polymer relaxation time to the neat solvent relaxation time.[9] These two quantities could be linked by a single constant of proportionality Q_{poly} defined by $Q_{poly} = A_{poly}/\log[\tau_{poly}(c_{poly} \rightarrow 0,T)/\tau_{solv}(c_{poly} = 0,T)]$ (see eq 12). To assess the influence of c_2 on the value of Q_2, a series of plots of A_2 vs $\log[\tau_2(c_2,T)/\tau_1(c_2 = 0,T)]$ were constructed for the various concentrations, c_2. The Q_2 values obtained from forced linear fits through the origin are given in Table 3. It seems reasonable to assume that when $\tau_2(c_2,T) = \tau_1(c_2 = 0,T)$, A_2 would be zero. If the time scales of the motions of "solute" and "solvent" are the same, the dynamic constraints imposed upon the relaxing solvent units will be unaffected by the addition of the solute and $A_2 = 0$.

It was assumed by Ngai and Rizos that $Q_{pi} = Q_{pve} = Q_{blend}$. It can be seen from Table 3 that this is not generally the case. In general, $Q_{pi} > Q_{pve}$. It is also seen from Table 3 that both Q_{pi} and Q_{pve} decrease as c_2 is increased. The decrease in Q_2 is not linear and predicting the value of Q_2 in the limit where $c_2 \rightarrow 0$ from measurements at higher concentrations may be complicated if not incorrect.

It seems reasonable that $Q_{pi} \neq Q_{pve}$ in light of the results from solution studies. Although Q_{poly} was found to be approximately equal for different polymers in the same solvent, differences in Q_{poly} were found when different solvents were considered (see Table 3).[9] Q_{pi} is obtained from an analysis in which PVE is treated as the solvent and Q_{pve} from an analysis in which PI is treated as the solvent. A change in Q_2 with changing solvent is consistent with the polymer solution studies.

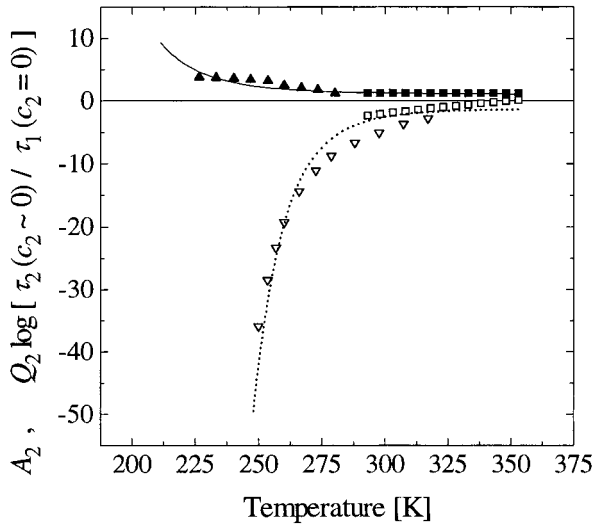

Figure 8. Comparison of the quantities A_2 and $Q_2 \log[\tau_2(c_2 \rightarrow 0,T)/\tau_1(c_2 = 0,T)]$. The solid and dotted lines represent the A_{pve} and A_{pi}, respectively, and are the solid and dotted lines of Figure 7. The solid symbols represent $Q_{pve} \log[\tau_{pve}(c_{pve} \rightarrow 0,T)/\tau_{pi}(c_{pve} = 0,T)]$ and the open symbols $Q_{pi} \log[\tau_{pi}(c_{pi} \rightarrow 0,T)/\tau_{pve}(c_{pi} = 0,T)]$. The squares represent the current optical data, and the triangles refer to the dielectric work of ref 10.

Figure 8 shows a plot comparing the temperature dependencies of A_2 and $Q_2 \log[\tau_2(c_2 \rightarrow 0)/\tau_1(c_2 = 0)]$. The dotted and solid lines represent A_{pi} and A_{pve}, respectively, and are equivalent to the dotted and solid lines of Figure 7. The open squares represent $Q_{pi} \log[\tau_{pi}(c_{pi} \rightarrow 0)/\tau_{pve}(c_{pi} = 0)]$ generated from the optical data. The solid squares represent the optical values of $Q_{pve} \log[\tau_{pve}(c_{pve} \rightarrow 0)/\tau_{pi}(c_{pve} = 0)]$. The dielectric data have again been included for comparison, represented by the open and solid triangles. It should be noted that the dielectric data were generated from the correlation times of blend compositions for which $c_2 > 0$ ($c_{pi} = 50\%$ and $c_{pve} = 25\%$). The Q_2 values used to shift the dielectric data are also given in Table 3. The temperature dependence of all the ratios, independent of c_2, does seem to be in reasonable agreement with the temperature dependence of the A_2 for both the 1 = PVE case and the 1 = PI case, although only the data for $c_2 \approx 0$ are shown.

Summary

Fluorescence anisotropy decay measurements of the component dynamics of PI:PVE blends have been performed. Correlation times are reported over the entire composition range for both components over the temperature range 20−100 °C. Measurements of the local dynamics of a probe molecule in a matrix that is ∼100% the second polymer species are reported for the first time. The temperature dependence of the blend components was found to be Arrhenius over this temperature range with different apparent activation energies for the different blend components.

The composition dependence of the PI and PVE components has been compared to the predictions of two blending rules proposed in this study. The composition dependence of the PVE component could be adequately described by an average of the correlation times of PVE* in bulk PVE and of PVE* in bulk PI weighted by the

blend composition. The composition dependence of the PI component could be accurately described by a parallel combination of the correlation times of PI* in bulk PI and PI* in bulk PVE again weighted by the blend composition. A closer inspection of the PVE component dynamics revealed that they were most accurately described by employing a linear combination of both the series (simple average) and parallel blending rules. This combination is such that the prefactors to the series and parallel contributions sum to one for all temperatures examined. The contribution from the series expression decreased as the temperature was increased.

Clearly, more work is required to test the validity and the significance of these proposed blending rules. Measurements within the PI:PVE system are needed covering the composition range from 25:75 to 0:100 and perhaps measurements closer to the blend T_g. It would also be interesting to observe whether the proposed blending rules are obeyed in other miscible polymer blends.

The data have also been analyzed in terms of equations developed to describe the modification of solvent dynamics in polymer solutions. The ratio of the time scales of the motions of the two polymers in the blend are found to be approximately proportional to the rate at which the addition of the second polymer modifies the dynamics of the first. The constant of proportionality is related to the strength of the coupling between the relative motions and is found to be both component and composition dependent.

Acknowledgment. We appreciate the helpful discussions with Dr. M. G. Brereton, Dr. K. Karatasos, and Prof. T. C. B. McLeish. We are indebted to Prof. R. Richards, Ms. A. Keeny, and Mr. T. Kiff of Durham University for the synthesis of the anthracene labeled polyisoprene. Financial support from the EPSRC (GR/K55486), the University of Leeds, and the Royal Society is gratefully acknowledged. S.A. thanks the University of Leeds for a university scholarship.

References and Notes

(1) Roovers, J.; Toporowski, P. M. *Macromolecules* **1992**, *25*, 1096.
(2) Colby, R. H. *Polymer* **1989**, *20*, 1275.
(3) Miller, J. B.; McGrath, K. J.; Roland, C. M.; Trask, C. A.; Garroway, A. N. *Macromolecules* **1990**, *23*, 4543.
(4) Zawada, J. A.; Fuller, G. G.; Colby, R. H.; Fetters, L. J.; Roovers, J. *Macromolecules* **1994**, *27*, 6861.
(5) Chung, G.-C.; Kornfield, J. A.; Smith, S. D. *Macromolecules* **1994**, *27*, 967, 5729.
(6) Takegoshi, K.; Tsuchiya, K.-I.; Hikichi, K. *Polym. J.* **1995**, *27*, 284.
(7) Arendt, B. H.; Krishnamoorti, R.; Kornfield, J. A.; Smith, S. D. *Macromolecules* **1997**, *30*, 1127.
(8) Ngai, K. L. *J. Polym. Sci., Polym. Phys.* **1991**, *29*, 867.
(9) Gisser, D. J.; Ediger, M. D. *Macromolecules* **1992**, *25*, 1284.
(10) Ngai, K. L.; Rizos, A. K. *Macromolecules* **1994**, *27*, 4493. Roland, C. M.; Ngai, K. L. *Macromolecules* **1991**, *24*, 2261.
(11) Roovers, J.; Toporowski, P. M. *Macromolecules* **1992**, *25*, 1096.
(12) Roland, C. M. *Macromolecules* **1987**, *20*, 2557.
(13) Roland, C. M.; Miller, J. B.; Mcgrath, J. J. *Macromolecules* **1989**, *22*, 256.
(14) Tomlin, D. W.; Roland, C. M. *Macromolecules* **1992**, 25, 2994.
(15) Hyde, P. D.; Ediger, M. D.; Kitano, T.; Ito, K. *Macromolecules* **1989**, 22, 2253 and references contained therein.
(16) O'Conner, D. V.; Philips, D. *Time-Correlated Single Photon Counting*; Academic Press: New York, 1984.
(17) Adams, S.; Adolf, D. B. *Macromolecules* **1998**, *31*, 5794.
(18) Viovy, J.-L.; Monnerie, L.; Brochon, J. C. *Macromolecules* **1983**, *16*, 1845.
(19) Vessier, V.; Viovy, J.-L.; Monnerie, L. *Polymer* **1989**, 30, 1262.
(20) Viovy, J.-L.; Monnerie, L.; Merola, F. *Macromolecules* **1985**, *18*, 1130.
(21) Hall, C. K.; Helfand, E. *J. Chem. Phys.* **1982**, *77*, 3275.
(22) Adolf, B. D.; Ediger, M. D.; Kitano, T.; Ito, K. *Macromolecules* **1992**, 25, 867.
(23) Waldow, D. A.; Ediger, M. D.; Yamaguchi, Y.; Matsushita, Y.; Noda, I. *Macromolecules* **1991**, *24*, 3147.
(24) Williams, M. L.; Landel, R. F.; Ferry, J. D. *J. Am. Chem. Soc.* **1955**, *77*, 3701.
(25) The tradition of plotting τ_c against $1/(T - T_g)$ is followed. It is understood, however, that this format does not necessarily reduce the data to an iso-free-volume state for blended systems. Problems relating to this have recently be highlighted by: Chapman, B. R.; Hamersky, M. W.; Milhaupt, J. M.; Kostelecky, C.; Lodge, T. P.; von Meerwall, E. D.; Smith, S. D. *Macromolecules* **1998**, *31*, 4562.
(26) Chapman, B. R.; Hamersky, M. W.; Milhaupt, J. M.; Kostelecky, C.; Lodge, T. P.; von Meerwall, E. D.; Smith, S. D. *Macromolecules* **1998**, *31*, 4562.
(27) Brereton, M. G. *Prog. Colloid Polym. Sci.* **1993**, *91*, 8.
(28) Lodge, T. P. *J. Phys. Chem.* **1993**, *97*, 1480.
(29) Fytas, G.; Rizos, A.; Floudas, G.; Lodge, T. P. *J. Chem. Phys.* **1990**, *93*, 5096.
(30) Alegria, A.; Colmenero, R.; Ngai, K. L.; Roland, C. M. *Macromolecules* **1994**, *27*, 4486.
(31) Roland, C. M.; Ngai, K. L. *Macromolecules* **1991**, *24*, 5315.

MA9816923